Article

Microscopic Mechanism for the Displacement of Shale Oil in a Nanochannel by CO_2 at Different Pressures

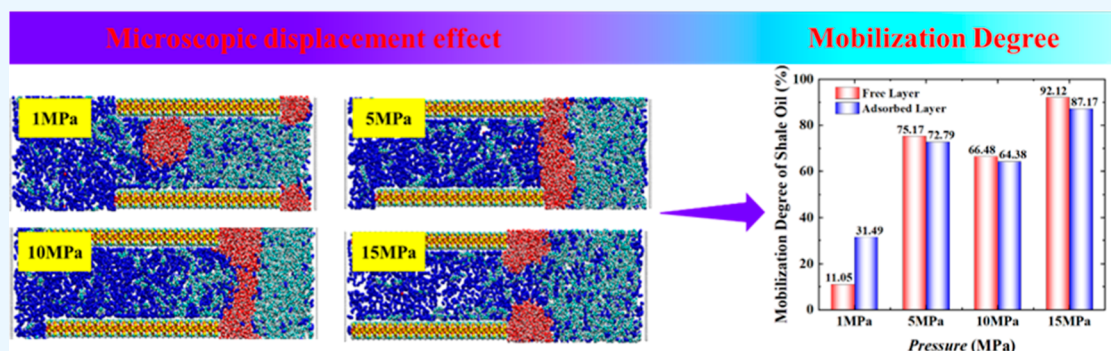Fengjiao Wang, Haiying Liao,* and Quanqi Dai

Read Online

ACCESS | Metrics & More | Article Recommendations

ABSTRACT: Aiming at the problems of unclear utilization degree of shale oil in different occurrence states. In this paper, the CO_2 displacement process of shale oil under different pressure conditions is simulated by the molecular dynamics method, the microscopic mechanism of CO_2 displacement of shale oil is clarified, and the influence of pressure on the utilization degree of different occurrence states of shale oil is revealed. The results show that CO_2 cannot form an effective flow channel under low pressure (1 MPa), and most of the oil and water remain in the channel. The water molecules form a water bridge at the outlet of the pore that CO_2 cannot break through under medium pressure conditions (5 and 10 MPa). CO_2 forms a stable flow channel under high pressure (15 MPa). With the increase of displacement pressure, the kinetic energy of oil and gas molecules in the channel increases. But limited by the system space, the diffusion capacity of shale oil system, the degree of oil and gas miscibility, and the competitive adsorption effect all show a trend of increasing first, then stabilizing, and rapidly increasing at last. The final recoveries of shale oil are 33.24%, 75.82%, 64.69%, and 83.03% under different displacement pressure conditions. Among them, the degree of oil and gas miscibility and shale oil utilization in the adsorbed layer is higher than that in the free layer under 1 MPa condition. And the shale oil utilization degree in the free layer is higher than that in the adsorbed layer under the other pressure conditions. This study can provide a theoretical basis for efficient development of shale oil.

1. INTRODUCTION

With the development of the global industry and the continuous reduction of conventional oil and gas resources, unconventional oil and gas resources represented by shale oil have gradually become a hot field of petroleum exploration and development.[1−3] With this background, CO_2 is considered to be a potential displacement medium due to its unique physical and chemical properties. Its low viscosity and high diffusivity enable CO_2 to effectively penetrate into the tiny pores of shale reservoirs and mix with shale oil, thus reducing the interfacial tension between oil and gas.[4−6] This process not only promotes the formation of miscible oil and gas but also reduces the viscosity of the crude oil, thus enhancing the fluidity of the shale oil.[7−9] In addition, CO_2 can also carry out competitive adsorption with shale oil in the pore, stripping the adsorbed shale oil on the surface of the pore, and further improving the shale oil recovery.[10]

Although CO_2 shows great potential in enhanced oil recovery, the displacement effect is still affected by many factors.[11−13] The complex pore size and wettability distribution in the shale reservoir lead to the difference in the interaction strength between shale oil and the surface. According to the interaction strength, shale oil can be divided into an adsorbed state and a free state. Among them, the adsorbed oil is tightly adsorbed on the surface due to the strong interaction, while the free oil mainly exists in the center of the channel due to weak interaction and is more easily displaced by CO_2.[14−16]

Displacement pressure is another key factor affecting the effect of CO_2 displacement.[17,18] Under high-pressure displacement conditions, CO_2 is endowed with a strong initial kinetic energy. This not only enhances the diffusion capacity of oil and gas molecules but also increases the miscibility between oil and gas. Moreover, it promotes the expansion of crude oil volume, thereby achieving efficient development of shale oil.[19,20] However, at present the research on the CO_2 displacement effect under different pressure conditions mainly focuses on the change of oil displacement efficiency, and the research on the utilization degree of adsorbed and free shale oil in pores is not clear.

In this paper, the CO_2 displacement shale oil model is established by a molecular dynamics simulation method. It elucidates the microscopic mechanism of the CO_2 displacement of shale oil and reveals the impact of pressure on the utilization degree of adsorbed and free shale oil. First, the occurrence states of shale oil in the channel were divided based on the density distribution curve, and the displacement process under different pressure conditions was investigated. Then, the microscopic mechanism of CO_2 displacement of shale oil is revealed from three aspects: diffusion capacity, miscibility, and competitive adsorption. Finally, the recovery of shale oil under different pressure conditions is determined, and the utilization degree of adsorbed and free state shale oil molecules is quantified.

2. MODEL AND METHODS

2.1. Model Construction. In order to determine the effect of displacement pressure on the ability of CO_2 displacement shale oil, methylated quartz was used to characterize the lipophilic surface of the channel. The surface model with the size of $24.54 \times 127.5 \times 11.30$ Å (1 Å = 0.1 nm) was formed by cutting the (0 0 1) surface of α-quartz and expanding the cell, the oxygen atoms on top of the quartz surface were methylated, and the oxygen atoms on the side of the quartz wall were hydroxylated to obtain the lipophilic surface with a total charge of 0. In addition, a shale oil system composed of $C_{12}H_{26}$ with a size of $24.54 \times 127.5 \times 23.44$ Å and a water system with a size of $24.54 \times 127.5 \times 5.73$ Å were constructed. The CO_2 system model with a size of $24.54 \times 70.54 \times 93.15$ Å and a He plate model with a size of $24.54 \times 70.54 \times 3$ Å were constructed. The above systems were combined and a 50 Å vacuum layer was added along the Z axis to avoid the influence of periodic boundary conditions on the simulation results.

2.2. Simulation Method. In this paper, LAMMPS was used to carry out molecular dynamics simulation, and VMD was used for molecular configuration visualization. The OPLS-AA force field was used to describe the thermodynamic and structural properties of alkane molecules, the EPM2 force field was used to describe CO_2 molecules, the SPC/E model was used to model water molecules, while the ClayFF force field was used to describe quartz walls. Periodic boundary conditions were used throughout the simulation, and the Nosé−Hoover thermostat was used to control the temperature at 353 K. The Coulomb potential was used to describe the long-range electrostatic interaction during the simulation, and the cutoff radius was set to 10 Å. The nonbond interaction in the model followed the Lennard−Jones potential (Figure 1). In order to ensure the stable distribution of shale oil, water, and CO_2 molecules in the system, before the formal displacement simulation, conjugate gradient algorithm was used to minimize energy treatment. In addition, NVT
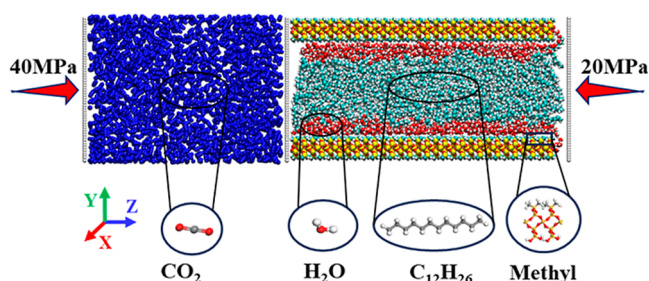

Figure 1. Initial conformation diagram of CO_2 displacement shale oil.

ensemble was used to carry out 2 ns equilibrium molecular dynamics simulation. The NVT ensemble can ensure that the number of atoms in the system and the volume and temperature of the system remain unchanged, and it is more suitable for shale oil and water molecules to fully adsorb on the pore wall, so as to simulate the real reservoir environment. When the temperature and energy of the system reach the equilibrium state, the model is considered to have reached the equilibrium state at this time, as shown in Figures 2 and 3.
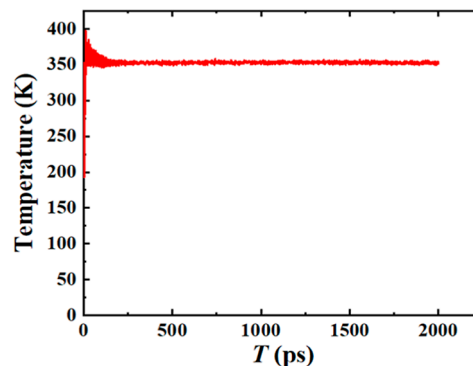

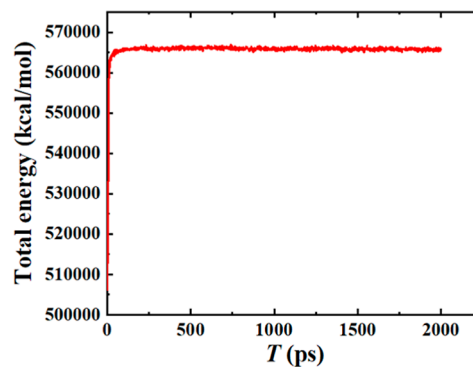**Figure 2.** Temperature equilibrium curve.

Figure 3. Pressure equilibrium curve.

Then a 40 MPa external force is applied to the He plate on the left side of the model along the Z axis, and a 20 MPa external force is applied to the He plate on the right side of the model to carry out the 5 ns CO_2 displacement process. The pressure conversion formula is as follows[21]

$$p = \frac{F \times N}{S_{xy}}$$

(1)

where p is the injection pressure, MPa; F is the external force, kcal/(mol Å); N is the total number of atoms in the nanopores; and S_{xy} is the area of the nanopores, Å^2.

3. RESULTS AND DISCUSSION

3.1. Distribution of Shale Oil.
The occurrence of oil and water molecules in the channel was simulated by equilibrium molecular dynamics, as shown in Figure 4. The water
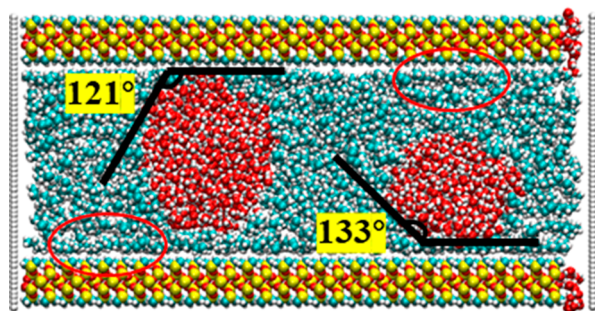

Figure 4. Distribution of shale oil in the pore.

molecules in the channel exist in the form of clusters, and the average contact angle between the water clusters and the wall surface reaches 127°, which is consistent with the actual wettability of the wall surface, indicating that the simulation in this paper has high credibility.[22,23] In addition, by drawing the density distribution curve of shale oil molecules along the Y axis direction, we further clarified the occurrence state of shale oil molecules in the pore, as shown in Figure 5. The density
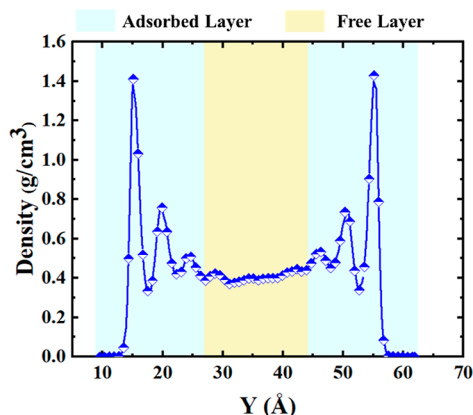

Figure 5. Density distribution curve of shale oil molecules along the Y axis.

distribution curve of shale oil molecules is symmetrical as a whole, and there are density fluctuation regions (9.5 ∼ 27.1, 44.3 ∼ 61.9 Å) and density stable regions (27.1 ∼ 44.3 Å) in the curve. Because the attraction of shale oil molecules on both sides of the surface is equal, and the closer the shale oil molecules are to the wall of the pore, the greater the attraction and the closer they are arranged, it shows obvious adsorption peaks on the density curve and is also called adsorbed shale oil molecules. The stable region on the curve represents the free shale oil molecules in the center of the pore. Due to the limited range of action of the wall, shale oil molecules in the central region of the pore are almost not attracted by the surface. Shale oil molecules float in the center of the pore, the density

distribution is approximately equal, and the corresponding density distribution curve tends to be stable.

3.2. Microscopic Migration Process of CO$_2$ Displacement of Shale Oil.
The displacement process under different pressure conditions (1, 5, 10, and 15 MPa) are shown in Figure 6. It can be seen from the figure that CO$_2$ will carry out the forward displacement and reverse imbibition processes at the same time, but there are obvious differences in the displacement phenomenon and utilization degree of CO$_2$ under different pressure conditions. Under the condition of 1 MPa pressure, there is no effective flow channel in the pore, and CO$_2$ will gradually disperse into the shale oil molecules and rely on reverse imbibition to replace the oil molecules in the pore; the degree of oil and water utilization in the pore is low. In contrast, CO$_2$ has a better displacement effect under the pressure conditions of 5 and 10 MPa. Due to the large pressure difference on both sides of the pore, CO$_2$ can form an effective flow channel. However, when the water molecular clusters are completely driven out of the channel, the water molecules are adsorbed at the outlet end under the action of the hydroxyl group on the side wall of the channel and gathered to form "water bridges" relying on the hydrogen bonding between water molecules. Since the pressure condition of 10 MPa can provide stronger initial kinetic energy for the water cluster, the migration speed of the water cluster is faster, and the "water bridge" can be formed earlier at the outlet of the channel, thus blocking the displacement process. As a result of the 15 MPa high-pressure displacement condition, water molecules at the outlet of the pore did not gather to form a "water bridge", and CO$_2$ formed a stable flow channel in the pore, which led to faster displacement of shale oil and higher utilization of shale oil.

3.3. Migration Mechanism of CO$_2$ Replacement of Shale Oil.
3.3.1. Self-Diffusion of Shale Oil. In order to clarify the diffusion capacity of shale oil components under different pressure conditions, the diffusion coefficients and volume changes of shale oil systems under the conditions of 1, 5, 10, and 15 MPa were statistically analyzed, as shown in Figures 7 and 8. The diffusion coefficients of shale oil components under different pressures (1, 5, 10, and 15 MPa) are 0.00163, 0.00323, 0.00321, and 0.01222 Å^2/ps, respectively. The volume changes were 2.986 × 10^4, 8.982 × 10^4 Å^3, 8.759 × 10^4, and 13.328 × 10^4 Å^3, respectively. The diffusion coefficient and volume change are 1< 5 ≈ 10 ≪ 15 MPa, showing a trend of increasing first and then maintaining a steady state, and then increasing sharply. Because the initial kinetic energy provided by the displacement pressure helps CO$_2$ drive more shale oil molecules to move, the diffusion ability of shale oil molecules in the pores is gradually enhanced and the distance between molecules is increased, so the volume expansion effect of crude oil is better. However, when the pressure rises to the "transition section" (5 and 10 MPa), although this pressure interval will push more CO$_2$ molecules into the pore, it is not enough to discharge shale oil molecules in time, resulting in limited diffusion space inside the pore. Therefore, the diffusion coefficient and volume change of shale oil components in the pressure interval of the "transition section" are approximately equal. Only when the pressure breaks through the range of the "transition section", the strong kinetic energy provided by the high pressure will promote the shale oil molecules to leave the pore in time, the diffusion coefficient will increase significantly, and the diffusion ability of shale oil molecules will increase sharply.
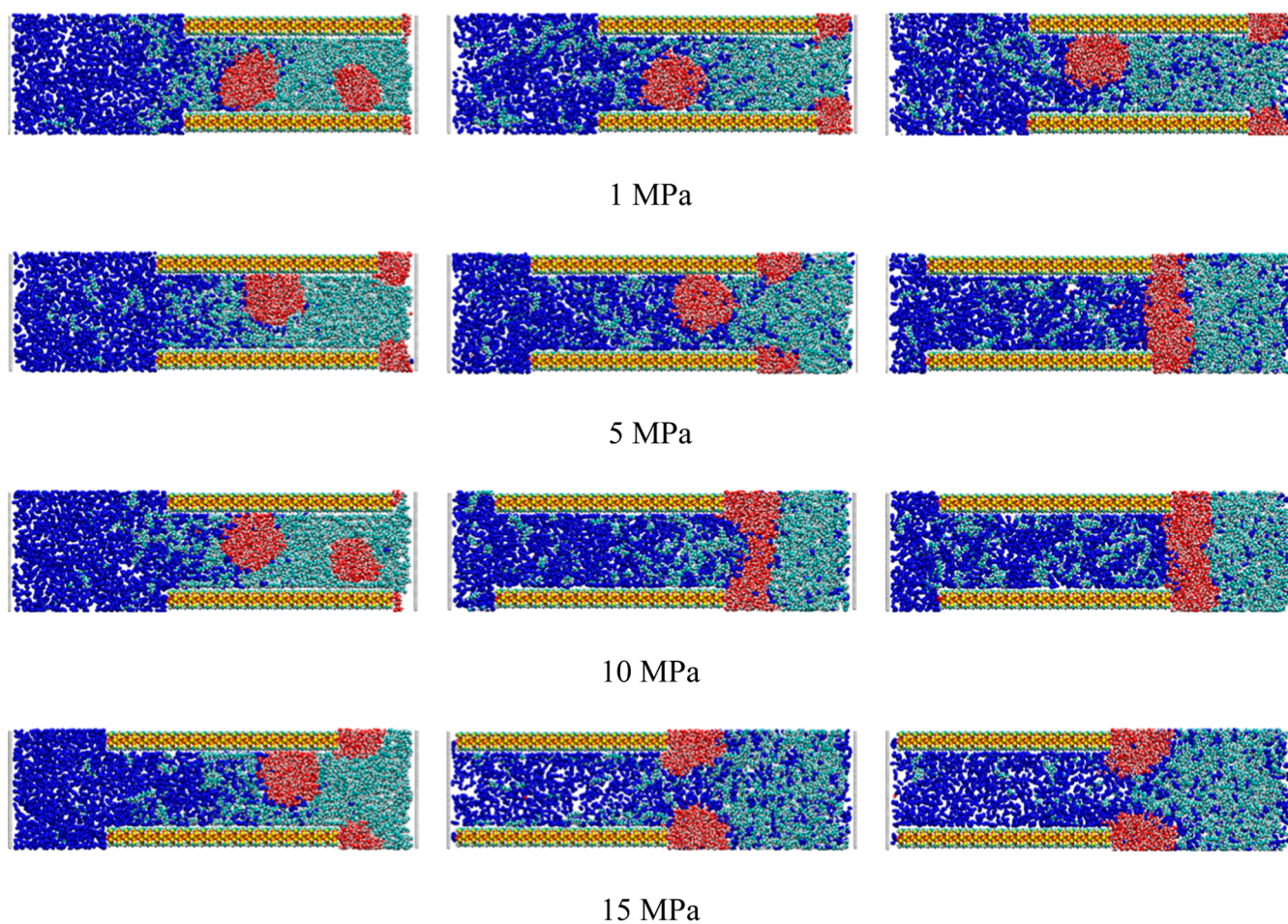
1 MPa

5 MPa

10 MPa

15 MPa

Figure 6. Migration process of CO_2 displacing shale oil at 1, 3, 5 ns under different pressure.

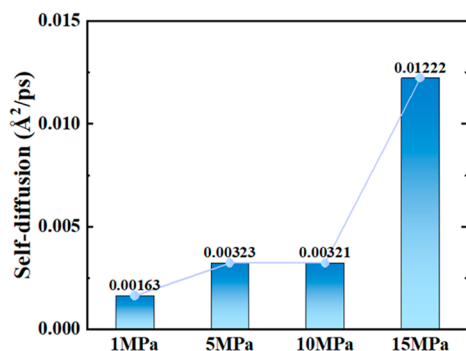**Figure 7.** Diffusion coefficients of shale oil systems under different pressure conditions.

Figure 8. Volume change of shale oil system under different pressure conditions.

3.3.2. Miscibility between CO_2 and Shale Oil.

In order to determine the degree of miscibility of oil and gas under different pressure conditions, the change in interaction energy between oil and gas components during displacement was analyzed. The greater the absolute value of the interaction energy, the stronger the interaction between oil and gas components and the closer the contact between oil and gas molecules. As shown in Table 1, with the progress of simulation, the absolute value of interaction energy between oil and gas molecules gradually increases, and the change rate of interaction energy gradually decreases. It shows that the degree of miscibility between oil and gas gradually increases and becomes stable with the process of displacement.
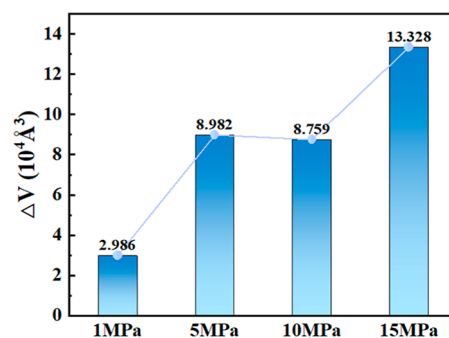
Table 1. Interaction Energy between CO_2-Shale Oil at Different Pressures and Different Stages (kcal/mol)

	1 MPa	5 MPa	10 MPa	15 MPa
1000 ps	−761.47	−724.829	−780.498	−781.732
2000 ps	−1123.75	−1018.71	−1108.69	−1220.04
3000 ps	−1318.23	−1250.38	−1316.34	−1486.14
4000 ps	−1439.77	−1447.02	−1442.96	−1667.21
5000 ps	−1601.2	−1505.88	−1540.01	−1783.6

However, comparing the interaction between oil and gas at 5000 ps under different pressure conditions, the following can be found: 15 MPa (−1783.6 kcal/mol) > 1 MPa (−1601.2 kcal/mol) > 10 MPa (−1540.01 kcal/mol) > 5 MPa
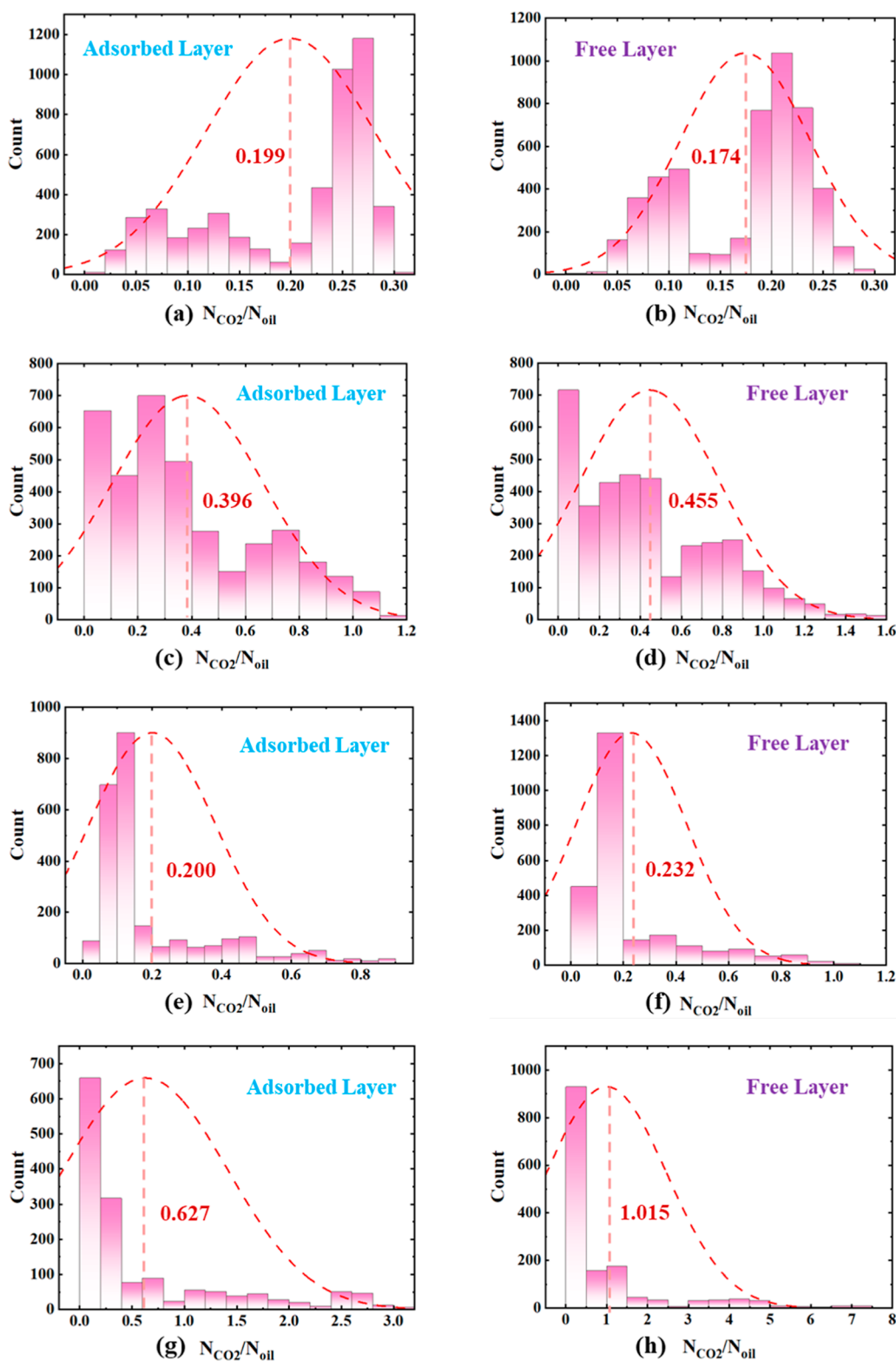
Figure 9. Proportion distribution of CO_2 and oil molecules in adsorbed layer and free layer under different pressure conditions. (a,b) 1; (c,d) 5; (e,f) 10; (g,h) 15 MPa.

(−1505.88 kcal/mol). Under the condition of 15 MPa, the degree of oil and gas miscibility is the highest, followed by 1 MPa, then 10 MPa, and finally 5 MPa. There is no linear relationship between the miscibility effect and the displacement pressure because CO_2 does not form an effective displacement channel under the displacement pressure of 1

MPa; CO_2 entering the pore cannot leave the pore but can only fully mix with shale oil molecules, and CO_2 gradually penetrates into the shale oil molecules, resulting in stronger interaction between oil and gas molecules and a higher degree of miscibility.

The degree of miscibility between CO_2 and shale oil in different states is further refined. Because CO_2 and alkane molecules are typical nonpolar molecules, there is no fixed charge distribution inside the molecules. When CO_2 enters the pore, it will be miscible with shale oil molecules by the action of intermolecular van der Waals forces. Thus, by separately tallying the ratio of CO_2 molecules to shale oil molecules within different regions, we can compare the degree of oil−gas miscibility. As shown in Figure 9, under different displacement pressure conditions (1, 5, 10, 15 MPa), the median relationship between the number ratios of CO_2 and oil molecules in the adsorbed layer and free layer was as follows: 1 MPa adsorbed layer (0.199) > 1 MPa free layer (0.174); 5 MPa free layer (0.455) > 5 MPa adsorption layer (0.396); 10 MPa free layer (0.232) > 10 MPa adsorption layer (0.200); 15 MPa free layer (1.015) > 15 MPa adsorbed layer (0.627). The closer the median value of the ratio between the number of CO_2 and oil molecules is to 1, the closer the number of oil and CO_2 molecules in the region and the stronger the degree of miscibility between oil and gas. The simulation results show that the degree of oil and gas miscibility of the adsorbed layer is higher than that of the free layer only under the condition of 1 MPa, and the degree of miscibility of the free layer is higher than that of the adsorbed layer under the conditions of 5, 10, and 15 MPa. Because the adsorbed shale oil molecules are more attracted by the surface, CO_2 will preferentially replace the free shale oil molecules, which are weakly attracted by the surface in the process of oil displacement, resulting in a higher degree of oil−gas miscibility in the free layer than that of the adsorbed layer. However, no complete flow channel has been formed in the pore under the condition of 1 MPa. As the external force is much stronger than the attraction effect of the wall on shale oil molecules, CO_2 entering the pore will disrupt the molecular arrangement of shale oil at the inlet indiscriminately. Since the adsorption layer region is much larger than the free layer region (35.2 ≫ 17.2 Å), the number of CO_2 molecules entering the adsorption layer is more and the degree of mutual solubility between oil and gas is higher.

3.3.3. Competitive Adsorption between CO_2 and Shale Oil. In order to clarify the competitive adsorption capacity of oil and gas components under different pressure conditions, the following formula is used to calculate the interaction energy and the difference between CO_2, shale oil molecules, and the wall surface.

$$E_{inter} = E_{total} - (E_{oil} - E_{surface}) \qquad (2)$$

where E_{inter} represents the interaction energy between shale oil and surface, kcal/mol; E_{total} represents the total energy of the system, kcal/mol; and E_{oil} and $E_{surface}$ represent the energy of oil and surface, kcal/mol, respectively.

The changes in the interaction energy are shown in Figures 10 and 11. With the increase of displacement pressure, the interaction energy between CO_2 and the surface shows an upward trend, while the interaction energy between shale oil and the surface shows a downward trend, and the difference of the interaction energy between the two is negative, indicating that CO_2 can peel the shale oil molecules adsorbed on the wall under the action of displacement pressure. However, the interaction energy differences under different displacement pressure conditions (1, 5, 10, and 15 MPa) are −28.434, −324.401, −325.491, and −424.352 kcal/mol, respectively. With the increase of displacement pressure, the difference of interaction energy also increases gradually, indicating that CO_2
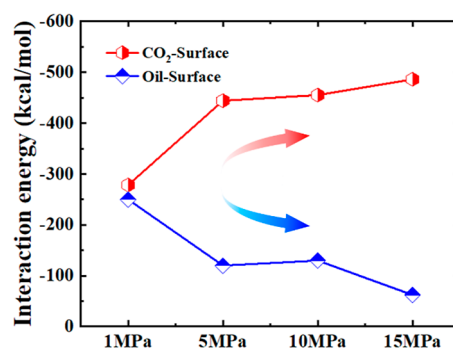

Figure 10. Interaction energy between CO_2 surface and oil surface.
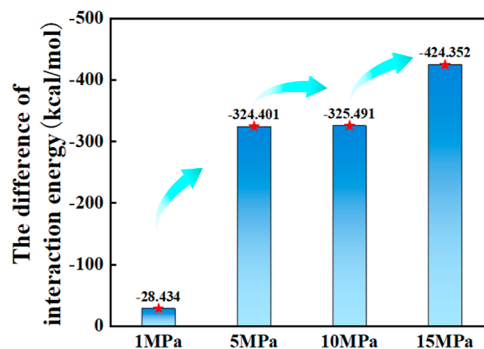

Figure 11. Interaction energy difference between CO_2 surface and oil surface.

has stronger stripping ability of shale oil molecules. This is because the more abundant the initial kinetic energy provided by high pressure for CO_2, the easier it is to push more CO_2 into pores to carry out competitive adsorption with shale oil molecules and the more effective it is to strip and replace the adsorbed shale oil molecules.

3.4. Evaluation of Oil Recovery and the Utilization Degree of Different Occurrence State Shale Oil. In order to clarify the impact of displacement pressure on shale oil recovery and different occurrence states of shale oil utilization, the relationship between the number of shale oil molecules inside the pore (adsorption layer and free layer) at the initial moment and the end of displacement is analyzed and quantified. The calculation formula is as follows

$$\eta = \frac{N_{total} - N_{residual}}{N_{total}} \qquad (3)$$

where η represents the recovery efficiency, N_{total} represents the total amount of shale oil molecules in the pore at the initial moment. $N_{residual}$ is the amount of shale oil remaining in the channel at the end of the displacement.

The variation of shale oil recovery under different displacement pressure conditions is shown in Figure 12. As can be seen from the figure, the recovery curve of shale oil shows a trend of first increasing and then stabilizing. The final recovery under different displacement pressure conditions (1, 5, 10, 15 MPa) reaches 33.24%, 75.82%, 64.69%, and 83.03%, respectively. The increase of displacement pressure will not only promote the oil and gas miscibility process but also improve the efficiency of CO_2 stripping to replace shale oil molecules, so the increase of displacement pressure will improve the CO_2 recovery. However, the recovery of shale oil under the condition of 10 MPa is lower than that under the condition
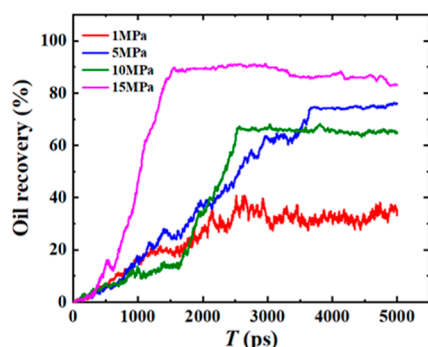
Figure 12. Shale oil recovery under different pressure conditions.

of 5 MPa because the 10 MPa condition provides more sufficient displacement power for CO_2 and the speed of oil and water molecules in the CO_2 displacement channel is faster. As the water molecular clusters are completely driven out of the channel, they will form a "water bridge" at the exit of the channel, resulting in the remaining shale oil molecules remaining in the channel; thus, the recovery rate of shale oil is reduced.

The variation of the utilization degree of adsorbed and free shale oil under different displacement pressures is shown in Figure 13. As can be seen from the figure, 1 MPa adsorbed
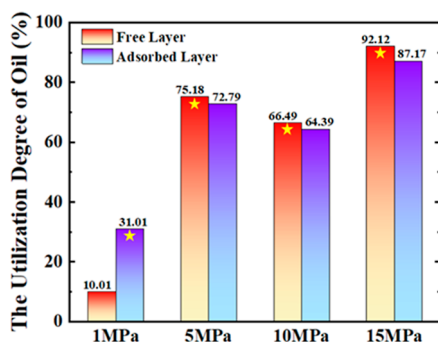

Figure 13. Utilization degree of adsorbed and free shale oil in pores under different pressure conditions.

layer (31.09%) > 1 MPa free layer (10.01%); 5 MPa free layer (75.18%) > 5 MPa adsorbed layer (72.79%); 10 MPa free layer (66.49%) > 10 MPa adsorption layer (64.39%); 15 MPa free layer (92.12%) > 15 MPa adsorbed layer (87.17%). The utilization degree of adsorbed oil is higher under 1 MPa, and the utilization degree of free oil is higher under other pressure conditions. Because the molecular arrangement at the inlet of the pore will be disturbed to a greater extent under the condition of 1 MPa, the degree of solubility in the adsorption layer region is higher than that in the free layer region and more CO_2 enters the adsorption layer region to replace and strip shale oil molecules, so the degree of shale oil utilization in the adsorption layer region is higher than that in the free layer.

4. CONCLUSIONS

In this paper, the CO_2 displacement process of shale oil under different pressure conditions is simulated by the molecular dynamics method, the occurrence state of shale oil in the channel delineated, and the microscopic mechanism of CO_2 displacement of shale oil analyzed in terms of diffusion capacity, miscibility, and competitive adsorption. On this basis,

the variation law of shale oil recovery under different pressure conditions is clarified, and the influence of pressure on the utilization degree of adsorbed and free shale oil is revealed. The main conclusions of this paper are as follows:

(1) CO_2 cannot form an effective flow channel under low pressure (1 MPa), and most of the oil and water remain in the channel; the water molecules form a water bridge at the outlet of the pore that CO_2 cannot break through under medium pressure conditions (5, 10 MPa). And CO_2 forms a stable flow channel under high pressure (15 MPa).

(2) With the increase of displacement pressure, the molecular kinetic energy of oil and gas in the pore increases but is limited by the system space; the diffusion coefficient of shale oil components, the degree of oil and gas miscibility, and the competitive adsorption effect all show a trend of increasing first, then stabilizing, and then rapidly increasing.

(3) Under different displacement pressure conditions (1, 5, 10, 15 MPa), the final recovery of shale oil is 33.24%, 75.82%, 64.69%, and 83.03%, respectively. The increase of displacement pressure will improve the effect of oil and gas miscibility and CO_2 stripping replacement of shale oil. However, the premature formation of the water bridge will limit the oil displacement efficiency of CO_2.

(4) Under the low pressure condition, CO_2 disturbs the molecular arrangement at the inlet of the channel, which leads to the higher degree of miscibility and shale oil utilization in the adsorbed layer than that in the free layer, and the free shale oil utilization is higher than the adsorption layer under the other pressure conditions.

■ AUTHOR INFORMATION

Corresponding Author

Haiying Liao − *National Energy Shale Oil Research and Development Center, Beijing 102206, P R China; Sinopec Petroleum Exploration and Production Research Institute, Beijing 100083, P R China;* orcid.org/0000-0003-3924-9738; Email: liaohy.syky@sinopec.com

Authors

Fengjiao Wang − *National Energy Shale Oil Research and Development Center, Beijing 102206, P R China; Sinopec Petroleum Exploration and Production Research Institute, Beijing 100083, P R China; Key Laboratory for Enhanced Oil & Gas Recovery of the Ministry of Education, Northeast Petroleum University, Daqing, Heilongjiang 163318, China;* orcid.org/0000-0001-8414-3049

Quanqi Dai − *National Energy Shale Oil Research and Development Center, Beijing 102206, P R China; Sinopec Petroleum Exploration and Production Research Institute, Beijing 100083, P R China*

Complete contact information is available at:
https://pubs.acs.org/10.1021/acsomega.4c10625

Notes

The authors declare no competing financial interest.

■ REFERENCES

(1) Feng, Q.; Xu, S.; Xing, X.; Zhang, W.; Wang, S. Advances and challenges in shale oil development: A critical review. *Adv. Geo-Energy Res.* **2020**, *4* (4), 406−418.

(2) Wang, F.; Liu, L.; Xu, H.; Liu, Y.; Meng, X.; Peng, B. An analytical solution model of oil-water dynamic imbibition considering dynamic contact angle effect and osmotic pressure at micro-nano scale. *Fuel* **2025**, *379*, 132979.

(3) Wang, F.; Xu, H.; Wang, S.; Deng, J.; Wang, Y. Fluid flow and efficient development technologies in unconventional reservoirs: State-of-the-art methods and future perspectives. *Adv. Geo-Energy Res.* **2024**, *12* (3), 237−240.

(4) Xiong, C.; Li, S.; Ding, B.; Geng, X.; Zhang, J.; Yan, Y. Molecular insight into the oil displacement mechanism of gas flooding in deep oil reservoir. *Chem. Phys. Lett.* **2021**, *783*, 139044.

(5) Luan, Y.; Liu, B.; Hao, P.; Zhan, K.; Liu, J. Oil displacement by supercritical CO_2 in a water cut dead-end pore: Molecular dynamics simulation. *J. Pet. Sci. Eng.* **2020**, *188*, 106899.

(6) Dong, X.; Xu, W.; Liu, H.; Chen, Z.; Lu, N. Molecular insight into the oil displacement mechanism of CO_2 flooding in the nanopores of shale oil reservoir. *Pet. Sci.* **2023**, *20* (6), 3516−3529.

(7) Wu, Z.; Sun, Z.; Shu, K.; Jiang, S.; Gou, Q.; Chen, Z. Mechanism of shale oil displacement by CO_2 in nanopores: A molecular dynamics simulation study. *Adv. Geo-Energy Res.* **2024**, *11* (2), 141−151.

(8) Sun, L.; Jia, N.; Feng, C.; Wang, L.; Liu, S.; Lyu, W. Exploration of Oil/Water/Gas Occurrence State in Shale Reservoir by Molecular Dynamics Simulation. *Energies* **2023**, *16* (21), 7253.

(9) Dou, X.; Zhu, P.; Qi, G.; He, Y.; Shao, D.; Qian, K. Mechanism for the Displacement of Shale Oil by CO_2 in Organic Nanopores. *Energies* **2022**, *15* (19), 7064.

(10) Sun, Y.; Zhang, W.; Tian, J.; Meng, Y.; Zhang, L. Research Progress on Displacement Mechanism of Supercritical CO_2 in Low-Permeability Heavy Oil Reservoir and Improvement Mechanism of Displacement Agents. *Molecules* **2023**, *28* (16), 6154.

(11) Liu, F.; Gao, X.; Du, J.; Lin, L.; Hou, D.; Luo, J.; Zhao, J. Microscopic mechanism of enhancing shale oil recovery through CO_2 flooding- insights from molecular dynamics simulations. *J. Mol. Liq.* **2024**, *410*, 125593.

(12) Wang, L.; Zhang, Y.; Zou, R.; Zou, R.; Huang, L.; Liu, Y.; Meng, Z.; Wang, Z.; Lei, H. A systematic review of CO_2 injection for enhanced oil recovery and carbon storage in shale reservoirs. *Int. J. Hydrogen Energy* **2023**, *48* (95), 37134−37165.

(13) Cheng, Y.; Lu, X.; Li, Q.; Liu, X. Molecular Insights into the Salinity Effects on Movability of Oil-Brine in Shale Nanopore-Throat Systems. *Langmuir* **2023**, *39* (46), 16494−16502.

(14) Wang, F.; Chang, S. Molecular dynamics investigation of shale oil occurrence and adsorption in nanopores: Unveiling wettability and influencing factors. *Chem. Eng. J.* **2024**, *481*, 148380.

(15) Wang, F.; Xu, H.; Liu, Y.; Meng, X.; Liu, L. Mechanism of Low Chemical Agent Adsorption by High Pressure for Hydraulic Fracturing-Assisted Oil Displacement Technology: A Study of Molecular Dynamics Combined with Laboratory Experiments. *Langmuir* **2023**, *39* (46), 16628−16636.

(16) Zhou, R.; Zhang, D.; Cheng, H.; Jin, T.; Ye, P.; Wei, J. Molecular dynamics study on hydration characteristics of expansive clay minerals by temperature and inorganic salts. *J. Mol. Liq.* **2024**, *409*, 125508.

(17) Hajianzadeh, M.; Mahmoudi, J.; Sadeghzadeh, S. Molecular dynamics simulations of methane adsorption and displacement from graphenylene shale reservoir nanochannels. *Sci. Rep.* **2023**, *13* (1), 15765.

(18) Zhang, J.; Gong, G.; Chen, K.; Zhang, Y.; Jiang, L.; Song, Y. Molecular Dynamic Simulation on the Dynamic Process of CH_4 Displacement by CO_2 in Shale Pores. *Energy Fuels* **2024**, *38* (8), 7057−7067.

(19) Zhang, S.; Zhang, Y.; Sun, X. Enhancement of Heavy Oil Recovery with High CO_2 Injection Rates in Silica Nanochannel. *Lithosphere* **2021**, *2021*, 3363280.

(20) Sun, J.; Chen, Z.; Wang, X.; Zhang, Y.; Qin, Y.; Chen, C.; Li, W.; Zhou, W. Displacement Characteristics of CO_2 to CH_4 in Heterogeneous Surface Slit Pores. *Energy Fuels* **2023**, *37*, 2926−2944.

(21) Sui, H.; Zhang, F.; Zhang, L.; Wang, Z.; Yuan, S.; Wang, D.; Wang, Y. Mechanism of CO_2 enhanced oil recovery in kerogen pores and CO_2 sequestration in shale: A molecular dynamics simulation study. *Fuel* **2023**, *349*, 128692.

(22) Xu, H.; Wang, F.; Liu, Y.; Meng, X.; Liu, L. Mechanism study on the influence of wettability on CO_2 displacement of shale oil in nanopores. *Fuel* **2024**, *376*, 132695.

(23) Wang, F.; Meng, X.; Xu, H.; Liu, Y.; Liu, L. Microscopic mechanism of CO_2 imbibition on mixed-wetting surface of shale oil reservoir. *Fuel* **2025**, *381* (D), 133592.